Frequency Spectrum of the Intracardiac and Body Surface ECG during Ventricular Fibrillation – a Computer Model Study

CN Nowak[1], G Fischer[1], L Wieser[1], B Tilg[1], HU Strohmenger[2]

[1]University for Health Sciences, MI and Technology, Hall, Austria
[2]Medical University, Innsbruck, Austria

Abstract

Recent findings indicate that stable organized centers of rapid activity (mother rotors) are the maintaining mechanism of ventricular fibrillation (VF). A computer model study was performed for understanding how intracardiac cellular activity is reflected at the body surface. The model contained a driving region of fast periodic activity (22 Hz). On the intracardiac layer the dominant frequency (DF) map revealed a constant DF of 22 Hz in the region of the mother rotor. A sharp drop of frequency (2 Hz - 12 Hz) occurred in the surrounding tissue of chaotic fibrillatory conduction. No organized pattern was observable on the body surface and the DF was reduced to 4.6 Hz - 8.5 Hz. It was shown that wave propagation transforms the spatial low pass filtering of the thorax into a temporal low pass in the far field. It hampers the observation of intracardiac organization from the body surface. No RC low pass was included in the model.

1. Introduction

The majority of sudden cardiac arrest is caused by ventricular fibrillation (VF) [1]. But still, the mechanisms underlying VF are poorly understood, because the ECG recorded on the body surface displays only a stochastic signal behaviour during VF. Thus, VF is traditionally described as a system of many chaotic in the myocardium wandering, electrical wavelets, ever changing in direction and number [2]. In contrast, recent findings indicate that stable organized centres of rapid activity, called "*mother rotors*", are the mechanism of maintaining VF [3]. Furthermore the characteristic chaotic appearance of VF is composed by the wavelets that emanate from the organized centre and interact with anatomical and functional obstacles. To verify this new hypothesis Samie et al. compared the results of a basic 2D computer model of cardiac tissue with measured intracardiac data from Langendorff perfused guinea pig hearts [3].

In the present report, a similar model as used by Samie et al. was applied for investigating how local organized activity is reflected on the body surface. For this reason a third dimension was added to the quadratic geometric yielding a cubic structure. This enables a comparison of intracardiac and body surface potentials. To show the differences between the cardiac tissue and the body surface in detail, the propagation of a plane wavefront on the one hand and of a mother rotor on the other hand was simulated on the cardiac tissue. So it can be demonstrated that the thorax as a volume conductor acts like a spatial-temporal filter, which damps high frequency components on the skin, even without including a resistive-capacitive (RC) low-pass filter in the model.

2. Methods

2.1. Computer model

Based on Samie et al.´s 2D computer model, a simplified 3D model, a 6 x 6 x 3.15 cm^3 cuboid, is developed. This model is subdivided into a 6 x 6 x 0.15 cm^3 section, representing cardiac tissue and a 6 x 6 x 3 cm^3 section, representing the thoracic volume conductor. The Luo-Rudy model phase-I [4] is used to specify the ionic currents in the cardiac tissue and the monodomain equation is applied for calculating the membrane potential [5]. To calculate the extracellular potential of the whole model, the second bidomain equation is used [5]. Moreover homogeneous Neumann boundary conditions are applied on the surface of the cuboid.

The normal pulse propagation (plane wavefront) was induced at the cardiac tissue by stimulating a whole edge of the tissue model. The mother rotor was produced by local action potential shortening (high potassium conductivity, low calcium conductivity) in the middle of the cardiac tissue (*"organized region"*).

For simulating the intracardiac and the body surface ECG, Einthoven's triangle is used to define three electrode positions for recording data on the cuboid. These three ECG electrodes are arranged each around the centre of top of the cuboid ("*skin layer*") and of the top of the cardiac tissue ("*intracardiac layer*") at a distance of 25 mm and an angle of 120° to each other. A central electrode is set in the middle of the skin layer and also the

endocardium. The unipolar potential was referenced such that a Wilson central terminal (WCT) defines zero [6].

2.2. Signal processing

For treating the simulated ECGs analogously to real data, they had to be pre-processed: For this reason, the signals were filtered by a 3 to 40 Hz Butterworth band-pass filter of order four and down sampled to 100 Hz.

Furthermore, for investigating the spectral components of the signal, the spectrum was calculated by using autoregressive modelling (AR). Model parameters were calculated through the Yule-Walker algorithm [7]. To select the best model order, the Akaike information criterion (AIC) is minimized [7]. The power spectral density (PSD) of the AR process is estimated by

$$PSD(f) = \frac{1}{f_s} \cdot \frac{\tilde{\sigma}^2}{\left| 1 + \sum_{n=1}^{N} \tilde{a}_n e^{-j2\pi n \frac{f}{f_s}} \right|^2}.$$

Where f_s is the sampling rate, $\tilde{a}_n$ are the estimated AR model parameters and $\tilde{\sigma}^2$ is the estimated white noise variance [8] at the AR model input. The frequency with the maximum PSD is termed dominant frequency (DF).

3. Results

3.1. Mother rotor

Using a cross-shock-protocol, a stable rotor could be induced with a frequency of 22 Hz in the middle of the cardiac tissue. The simulation lasts 3 s with a sampling rate of 1000 Hz.

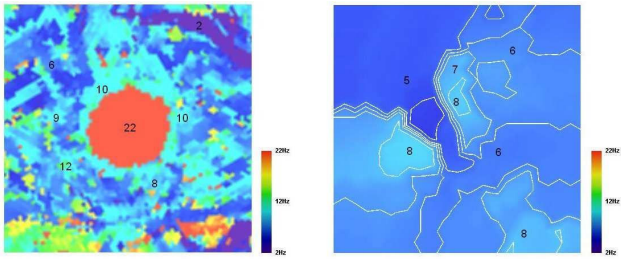

(a) Intracardiac (b) Skin

Figure 1. Dominant frequency maps. The dominant frequencies range between 2 Hz and 22 Hz at the intracardiac (a) and between 4.6 Hz to 8.5 Hz at the skin layer (b) of the model.

For getting a general overview of the appearance of the frequency components in the computer model, a dominant frequency (DF) map of the two layers of interest (intracardiac layer and skin layer) is calculated as can be seen in fig 1. Figure 1a shows that the stable rotor in the middle of the intracardiac layer is responsible for the highest DF. In all the rest of this layer it can be seen that the pattern of the map is chaotic. The DF varies between 2 Hz and 15 Hz. This pattern is caused by many wavelets of a short lifespan that emerge from the stable rotor. Figure 1b shows the DF map on the skin layer. Due to the small variation in DF isolines are plotted. No organized region can be observed anymore. Moreover, the DF values only range between 4.6 Hz and 8.5 Hz. Contrary to the epicardium, the DF map of the skin layer is smoother.

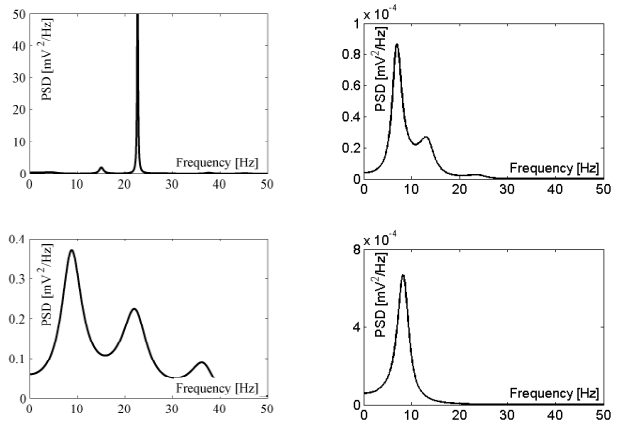

(a) Intracardiac (b) Skin

Figure 2. Comparison of the unipolar ECG and the PSDs of (a) the intracardiac and (b) the skin layer.

Furthermore, the unipolar ECG during VF is recorded and for investigating the differences between the intracardiac and the skin layer the spectra were calculated by using AR estimation:

Figure 2a shows the PSDs of both the organized (upper panel) and the region with the chaotic pattern (lower panel) of the intracardiac layer. The signal of the upper panel is measured from the central lead and the signal of the lower panel is measured from one electrode (#1) of the Einthoven´s triangle. The mean model order of the organized region amounts 38 and it is 19 (range 14 to 24) for the chaotic region of the signals from the intracardiac layer. The mean AR model order is 23 in the organized region and 22 in the chaotic region at the skin layer.

In the organized region, one high peak was measurable at 22 Hz with an amplitude of $58.44 \cdot 10^{-3}$ V^2/Hz. This high peak represents the stable rotor in the middle of the layer. In the PSD of lead 1 three peaks can be recognized at 8.8 Hz with an amplitude of $0.37 \cdot 10^{-3}$ V^2/Hz, at 22 Hz with an amplitude of $0.22 \cdot 10^{-3}$ V^2/Hz and at 36.1 Hz with an amplitude of $0.09 \cdot 10^{-3}$ V^2/Hz. The stable rotor caused the frequency component at 22 Hz. The first peak at 8.8

Hz originated from the wavelets wandering in the chaotic region. Overtones of the signal components from the chaotic region compose the third peak.

Figure 2b shows the PSDs of the organized (upper panel) and the chaotic (lower panel) region of the skin layer. Again, the signal of the upper panel is measured from the central lead and the signal of the lower panel is measured from one electrode (#1) of the Einthoven´s triangle. The frequency spectrum of the central lead consists of three peaks at 6.9 Hz, and 13 Hz to 22.4 Hz with amplitudes of $86.64 \cdot 10^{-6}$ V^2/Hz, $26.88 \cdot 10^{-6}$ V^2/Hz and $2.72 \cdot 10^{-6}$ V^2/Hz. The signal measured from the electrode in the chaotic has only one peak at 7.1 Hz with an amplitude of $0.88 \cdot 10^{-3}$ V^2/Hz. It is remarkable that only in the spectrum of the central lead, a frequency component at 22 Hz is recognizable. In no signal of the three other electrodes of the skin layer this frequency component is measurably. The results suggest that the thoracic volume conductor might act as a spatial-temporal low-pass filter.

3.2. Plane wavefront

For confirming the observation that the thoracic volume conductor acts as a spatial-temporal filter, normal pulse propagation (plane wavefront) is induced at the cardiac tissue by stimulating one whole edge of the tissue model. A time interval of 130 ms duration was simulated. The data was sampled with a rate of 1000 Hz. The median frequency is 138±16 Hz in the intracardiac layer, while a median frequency of 4.2±0.9 Hz is obtained at the skin layer. That means that there is a great attenuation between the two layers.

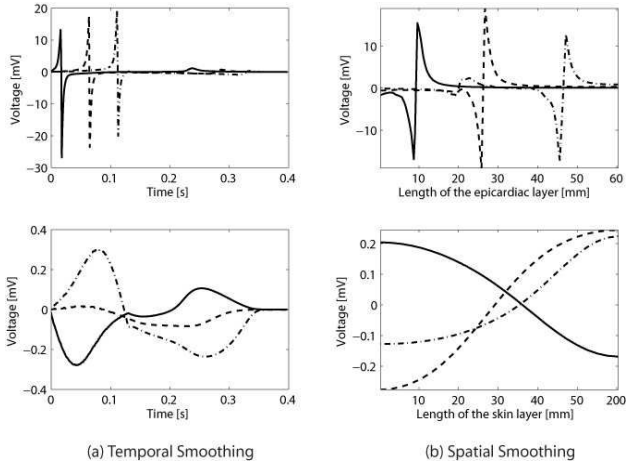

Figure 3. The signals of the three electrodes of the intracardiac layer (upper panel) in opposite to the skin layer (lower panel) are shown in (a). The electrical activity of the intracardiac (upper panel) and the skin (lower panel) layer along the model at three different times (20 ms,57 ms and 100 ms) is shown in (b).

The upper panel of fig. 3a shows the signals of the three Einthoven electrodes at the cardiac tissue. The duration between the maximum and the minimum of the signal amounts 1.7±0.5 ms. In contrast to the intracardiac ECG, the peak-to-peak duration of the skin ECG is 193±15.8 ms, as can be seen in the lower panel of fig 3a.

Figure 3b shows the spatial smoothing of the signals comparing the intracardiac (upper panel) and the skin (lower panel) layer at three different times: The solid lines show the potential at 20 ms, the dotted lines at 57 ms and the dashed lines at 100 ms. The potential is plotted along a straight line in the middle of the layer. The line is oriented in parallel with the direction of propagation. The absolute value of the peak-to-peak distances is shorter in the cardiac tissue (1.2±0.3 mm) than on the body surface (58.7±5.9 mm). That indicates that the potential maxima and minima on the skin layer lie on or close the boundary of the model (edge length 60 mm).

These results confirm the existence of a low-pass filter, but without integrating RC like structures in the model.

4. Discussion and conclusions

Based on the studies of Samie et al. that major organized centers are the driving source of maintaining VF, a simplified 3D computer model was developed to investigate if these mother rotors are reflected on the body surface and in the body surface ECG.

The surprising result of the present study shows that the high frequency components of the intracardiac ECG are damped on the body surface. Although the stable rotor has a frequency of 22 Hz the cardiac tissue, no pronounced 22 Hz component can be seen in the PSD of the body surface ECG. Only for unipolar recordings taken directly above the organized centre of VF, a small spectral peak with the frequency of the mother rotor was found. Especially frequency components above about 10 Hz are significantly damped on the skin. These observations leads to the finding that the thoracic volume conductor acts as a spatial – temporal low pass filter, that hampers the measurements of local organization from the body surface.

It is a remarkable fact that this filter effect can be recognized in the computer model, although no resistive-capacitive low pass filter is included in the volume conductor model. That means that this filter effect results only from an interaction of wave propagation and spatial smoothing in the far field.

To sum up, it has been shown that high frequency components of the cardiac activity are damped on the body surface because of the fact that the thoracic volume conductor acts as a spatial-temporal low pass filter. So it

is difficult to investigate the rapid, organized sources of VF from the body surface and to detect these high frequency components in the body surface ECG. Only the contributions from chaotic fibrillatory conduction dominate the non-invasively accessible signal. Future studies in an anatomically more accurate model should help to support the development of a non-invasive marker for guiding the countershock therapy in emergency case.

Acknowledgements

This study was supported by the Jubiläumsfonds of the Austrian National Bank under grant nr. 8599 and the Austrian Science Fund under grant P16579-N04.

References

[1] Strohmenger HU, Lindner KH, Brown CG. Analysis of the Ventricular Fibrillation ECG Signal Amplitude and Frequency Parameters as Predictors of Countershock Success in Humans. Chest 1997;111:584-589.

[2] Reed MJ, Clegg GR, Robertson CE. Analysing the ventricular fibrillation waveform. Resuscitation 2003;57:11-20 .

[3] Samie FH, Berenfeld O, Anumonwo J, Mironov SF, Udassi S, Beaumont J, Taffet S, Pertsov AM, Jalife J. Rectification of the background potassium current: a determinant of rotor dynamics in ventricular fibrillation. Circ Res 2001;89:1216-1223.

[4] Luo CH, Rudy Y. A model of the ventricular cardiac action potential. Depolarization, repolarization, and their interaction. Circ Res 1991;68:1501-1526.

[5] Vigmond EJ, Aguel F, Trayanova NA. Computational techniques for solving the bidomain equations in three dimensions. IEEE Trans Biomed Eng 2002;49:1260-1269.

[6] Fischer G, Tilg B, Modre R, Hanser F, Messnarz B, Wach P. On modelling the Wilson terminal in the boundary and finite element method. IEEE Trans Biomed Eng 2002;49:217-224.

[7] Stoica P, Moses RL. Introduction to Spectral Analysis. Prentice-Hall (Engelwood Cliffs,New Yersey), 1997.

[8] Baselli G, Porta A, Rimoldi O, Pagani M, Cerutti S. Spectral decomposition in multichannel recordings based on multivariate parametric identification. IEEE Trans Biomed Eng 1997;44:1092-1101.

Address for correspondence

Claudia-Nike Nowak
Institute for Biomedical Engineering
University for Health Sciences, MI and Technology
Eduard-Wallnoefer Zentrum 1
6060 Hall i.Tirol, Austria
claudia.nowak@umit.at